Excitation System by Contactless Power Transfer System with the Primary Series Capacitor Method

Ryosuke Nozawa, Ryota Kobayashi, Hikaru Tanifuji, Yasuyoshi Kaneko, Shigeru Abe
Department of Electrical and Electronic Systems
Saitama University
Saitama, Japan

***Abstract*—For power transfer to the rotor circuit of excitation-type synchronous motors, we propose a contactless power transfer system with a primary series capacitor (S topology) to compensate for the leakage reactance. This system does not contain secondary resonant and smoothing capacitors and can reduce the number of components in the rotor circuit. The value of the primary resonant capacitor is determined such that the input power factor is set to one for the operating frequency. The rotating shaft of the rotor is covered with an aluminum sheet to reduce the loss due to the leakage flux. Power transfer tests were performed. A high efficiency of 91.8% was achieved when power was transferred to the rotor circuit of the synchronous motor.**

Keywords—contactless power transfer system, electromagnetic shielding, rotary transformer, synchronous motor

I. INTRODUCTION

We study an excitation-type synchronous motor using a contactless power transfer system for the partial development of a variable magnetic flux motor. Conventionally, slip rings and a brushless excitation system have been used as the excitation method in excitation-type synchronous motors and generators. The slip ring is limited by the rotational speed and creates dust and wear during sliding because it has contact points. On the other hand, a brushless excitation system does not have contact points, but it is not able to excite the rotor at the start of operation. To overcome these problems, excitation using a contactless power transfer system has been proposed [1]–[5]. A contactless power transfer system has no limit to the rotational speed and does not create dust, wear, sparks, or contact failure. Further, the contactless power transfer system has the advantages of being clean and maintenance free and is able to excite the rotor of motor at the start of operation.

A contactless power transfer system using a rotary transformer has been used in a video deck, resolver, etc.; however, these systems are for dealing with small power such as signal transmission. When developing a contactless power transfer system for an excitation-type synchronous motor, it is necessary to consider miniaturizing and reducing the weight of the secondary circuit and loss due to the shaft of magnetic material. It is necessary for the secondary circuit to be small, lightweight, and maintenance free for mechanical strength and maintainability if it is placed in the interior of the rotor. A high-frequency magnetic field generated by a contactless power transfer system causes iron loss of the magnetic materials surrounding the transformers and decreases the transmission efficiency.

In this paper, we investigate the resonant capacitor topology for leakage reactance compensation and the omission of the smoothing capacitor, considering miniaturization and weight reduction of the secondary side. In addition, we also investigate the magnetic shielding of the shaft.

For the resonant capacitor topology, we examine the characteristics of the contactless power transfer system with a primary series resonant capacitor (S topology) and compare with the series and parallel capacitor topology (SP topology). In a contactless power transfer system with a large air gap for an electric vehicle, the SP topology is often used for leakage reactance compensation [6], [7]. On the other hand, the S topology is able to omit the secondary capacitor and achieve miniaturization and weight reduction of the secondary circuit. Using the S topology, we derive equations to calculate the value of the primary series capacitor C_{OS}, the maximum transformer efficiency η_{TRmax}, and its load resistance R_{Lmax}.

For omission of the smoothing capacitor, the inductance of the excitation windings around the rotor of the synchronous motor is used. The effectiveness of an aluminum sheet has been described to magnetically shield the motor shaft [8]. In order to determine the most effective shape for the aluminum shield for the S topology, we performed simulations and power transfer experiments.

II. CONTACTLESS POWER TRANSFER SYSTEM

A. Series and Parallel Resonant Capacitor Topology (SP Topology)

Fig. 1(a) shows a schematic diagram of the contactless power transfer system for the SP topology. A full-bridge inverter is used as a high-frequency (f_0 = 50 kHz) power supply. Fig. 1(b) shows a detailed equivalent circuit. The primary values are converted into secondary equivalent values using the turns ratio $a = N_1/N_2$. Because the winding resistances and ferrite-core loss are considerably lower than the mutual and leakage reactances at the resonant frequency, the winding resistances (r'_1 and r_2) and the ferrite-core loss r'_0

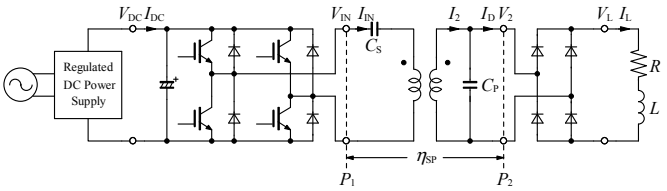

(a) Schematic diagram.

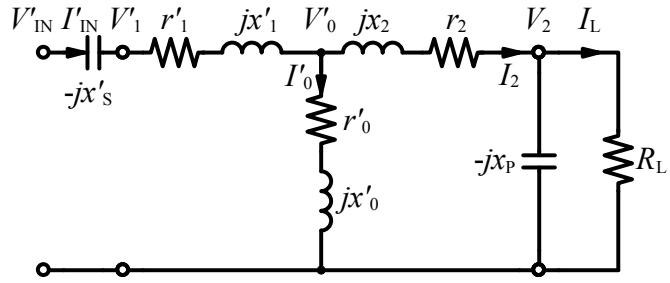

(b) Detailed equivalent circuit.

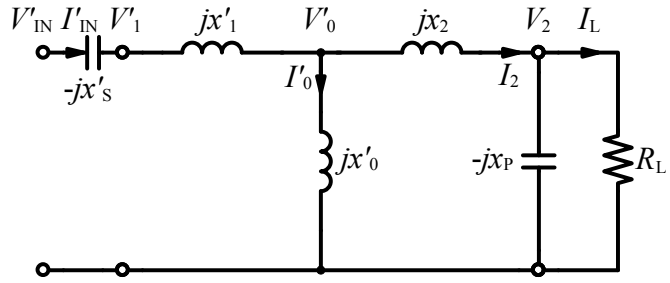

(c) Simplified equivalent circuit.

Fig. 1. Contactless power transfer system for the SP topology.

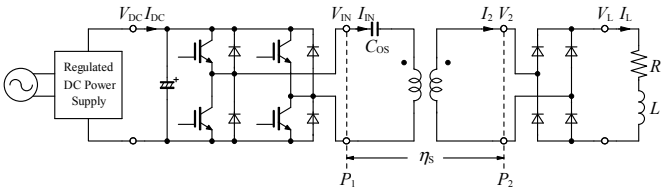

(a) Schematic diagram.

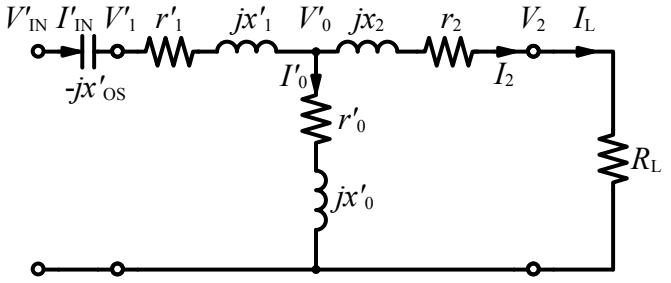

(b) Detailed equivalent circuit.

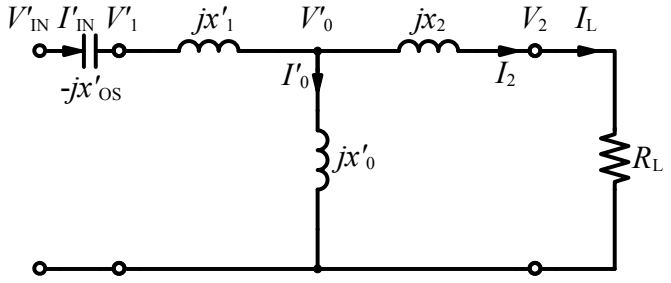

(c) Simplified equivalent circuit.

Fig. 2. Contactless power transfer system for the S topology.

can be ignored. Fig. 1(c) shows the simplified equivalent circuit that ignores r'_1, r'_2, and r'_0 from the detailed equivalent circuit.

To achieve resonance of the input frequency f_0 ($=\omega_0/2\pi$) with the self-inductance of the secondary winding L_2, which is equivalent to adding a mutual reactance x'_0 and a leakage reactance x_2, the secondary parallel capacitor C_P is given by

$$\frac{1}{\omega_0 C_P} = x_P = x'_0 + x_2 \tag{1}$$

The value of the primary series capacitor C_S (C'_S denotes its secondary equivalent) is determined when the imaginary part of the impedance is zero, and the inverter output power factor of the fundamental wave is to be one. C_S is given by

$$\frac{1}{\omega_0 C'_S} = x'_S = \frac{x'_0 x_2}{x'_0 + x_2} + x'_1 \tag{2}$$

The input voltage V'_{IN} and the input current I'_{IN} can be expressed as

$$V'_{IN} = bV_2, \quad I'_{IN} = I_L / b, \quad b = \frac{x'_0}{x'_0 + x_2} \tag{3}$$

These equations show that the equivalent circuit of a transformer with these capacitors is the same as an ideal transformer at the resonant frequency.

Ignoring r'_0, the efficiency of the transformer for the SP topology in Fig. 1(b) is defined by

$$\eta_{SP} = \frac{R_L I_L^2}{R_L I_L^2 + r'_1 I'^2_{IN} + r_2 I_L^2} = \frac{1}{R_L + \frac{r'_1}{b^2} + r_2\left\{1 + \left(\frac{R_L}{x_P}\right)^2\right\}} \tag{4}$$

The maximum transformer efficiency η_{maxSP} is obtained when $R_L = R_{LmaxSP}$.

$$R_{LmaxSP} = x_P \sqrt{\frac{1}{b^2}\frac{r'_1}{r_2} + 1} \tag{5}$$

$$\eta_{maxSP} = \frac{R_L}{1 + \frac{2r_2}{x_P}\sqrt{\frac{1}{b^2}\frac{r'_1}{r_2} + 1}} \tag{6}$$

The coupling factor k, the quality factor of the primary winding Q_1, and the quality factor of the secondary winding Q_2 are expressed as

$$k = \frac{M}{\sqrt{L_1 L_2}}, \quad Q_1 = \frac{\omega L_1}{r_1}, \quad Q_2 = \frac{\omega L_2}{r_2} \tag{7}$$

Then, the equations for R_{LmaxSP} and η_{maxSP} can be expressed in terms of k and Q.

$$R_{Lmax} = \frac{r_2 Q_2}{k}\sqrt{\frac{Q_2}{Q_1} + k^2} \tag{8}$$

$$\eta_{maxSP} = \frac{1}{1 + \frac{2}{k}\sqrt{\frac{1}{Q_1 Q_2} + \frac{k^2}{Q_1^2}}} \tag{9}$$

(a) External form.

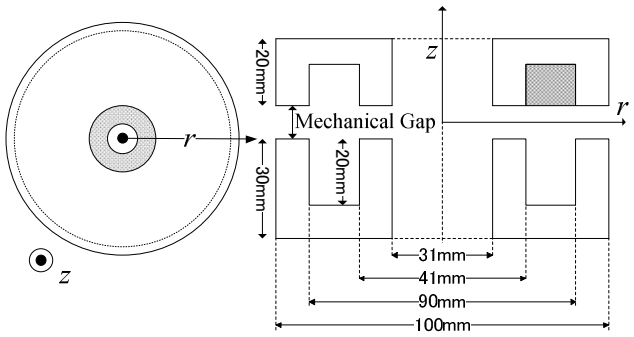

(b) Transformer dimensions.

Fig. 3. Rotary contactless power transformer.

TABLE I. TRANSFORMER SPECIFICATIONS

Rated power		1.0 kW
Mechanical gap		2 mm
Windings wires	Primary	24T1p
	Secondary	10T1p
Weight	Primary	890 g
	Secondary	610 g
Litz wire		0.1 mmφ × 800
Ferrite core		TDK PE90

B. Primary Series Capacitor Topology (S Topology)

Fig. 2(a) shows a schematic diagram of the contactless power transfer system for the S topology. A full-bridge inverter is used as a high-frequency (f_0 = 50 kHz) power supply. Fig. 2(b) shows a detailed equivalent circuit, and Fig. 2(c) shows the simplified equivalent circuit ignoring r'_1, r'_2, and r'_0 from the detailed equivalent circuit.

For the simplified equivalent circuit in Fig. 2(c), the impedance seen from the primary input is given by

$$Z = \frac{R_{\mathrm{L}} x_0'^2}{R_{\mathrm{L}} + (x_0' + x_2)^2} + j\left\{ \frac{x_0'\left[R_{\mathrm{L}}^2 + x_2(x_0' + x_2)\right]}{R_{\mathrm{L}}^2 + (x_0' + x_2)^2} + x_1' \right\} \tag{10}$$

The value of the primary series capacitor C_{OS} is determined when the imaginary part of the impedance is zero, and the inverter output power factor of the fundamental wave is to be one. C_{OS} is given by

$$\frac{1}{\omega_0 C_{\mathrm{OS}}'} = x_{\mathrm{OS}}' = \frac{x_0'\left[R_{\mathrm{L}}^2 + x_2(x_0' + x_2)\right]}{R_{\mathrm{L}}^2 + (x_0' + x_2)^2} + x_1' \tag{11}$$

Therefore, the relationship between the input and the output is expressed as

$$I_{\mathrm{IN}}' = -j\frac{1}{x_0'} V_{\mathrm{L}} + \frac{x_0' + x_2}{x_0'} I_{\mathrm{L}} \tag{12}$$

Ignoring r'_0, the efficiency of the transformer for the S topology in Fig. 2(b) is defined as

$$\eta_{\mathrm{S}} = \frac{R_{\mathrm{L}} I_{\mathrm{L}}^2}{R_{\mathrm{L}} I_{\mathrm{L}}^2 + r_1' I_{\mathrm{IN}}'^2 + r_2 I_{\mathrm{L}}^2} = \frac{R_{\mathrm{L}}}{\frac{r_1'}{x_0'^2}\left[R_{\mathrm{L}}^2 + (x_0' + x_2)^2\right] + R_{\mathrm{L}} + r_2} \tag{13}$$

TABLE II. TRANSFORMER PARAMETERS

Situation		With shaft and aluminum sheet (1.5 mm)			Without shaft
f_0 [kHz]		50			
gap [mm]		1	2	3	2
r_1 [mΩ]		188.1	103.3	85.6	88.6
r_2 [mΩ]		6.87	23.3	28.6	19.7
l_0 [μH]		123.8	110.1	101.1	185.8
l_1 [μH]		60.8	63.2	68.7	48.8
l_2 [μH]		8.46	8.80	8.80	8.97
k		0.70	0.67	0.64	0.79
Q_1		308	527	623	832
Q_2		1370	376	289	657
SP	C_{S} [μF]	0.106	0.103	0.099	0.114
	C_{P} [μF]	0.338	0.363	0.384	0.246
	R_{LmaxSP} [Ω]	30.1	14.26	12.2	19.53
	η_{maxSP} [%]	99.54	99.14	98.99	99.54
	η_{SP} [%]*	97.16 (99.42)	96.95 (99.14)	97.2 (98.97)	—
	pf_1*	0.88	0.91	0.93	—
	pf_2*	0.63	0.62	0.62	—
S	C_{OS} [μF]	0.071	0.072	0.071	0.071
	R_{LmaxS} [Ω]	9.91	11.13	11.28	17.3
	η_{maxS} [%]	98.60	98.91	98.91	99.48
	η_{S} [%]*	97.67 (98.60)	97.16 (98.90)	96.35 (98.90)	—
	pf_1*	0.82	0.81	0.77	—
	pf_2*	0.87	0.86	0.86	—

* experimental value
( ) Calculated value of efficiency
pf: power factor

The maximum transformer efficiency η_{maxS} is obtained when $R_{\mathrm{L}} = R_{\mathrm{LmaxS}}$.

$$R_{\mathrm{LmaxS}} = \sqrt{(x_0' + x_2)^2 + \frac{x_0'^2 r_2}{r_1'}} \tag{14}$$

$$\eta_{\mathrm{maxS}} = \frac{1}{1 + \frac{2r_1'}{x_0'^2}\sqrt{(x_0' + x_2)^2 + \frac{x_0'^2 r_2}{r_1'}}} \tag{15}$$

The equations for R_{LmaxS} and η_{maxS} expressed in terms of k and Q are as follows:

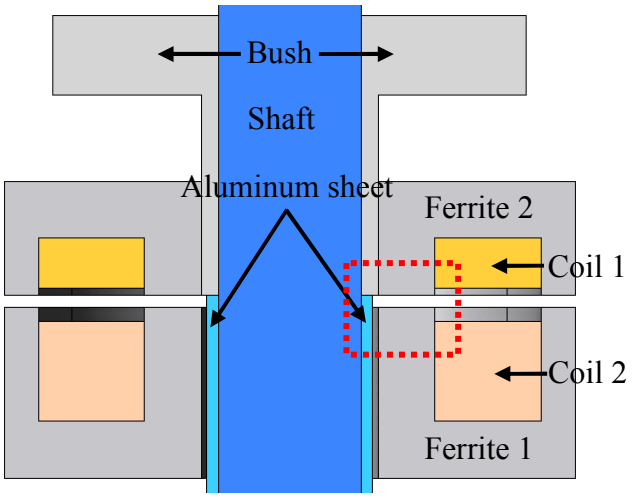

(a) Revolved section of the transformer.

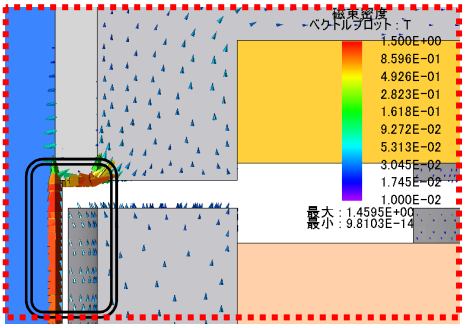

(b) Without an aluminum sheet.

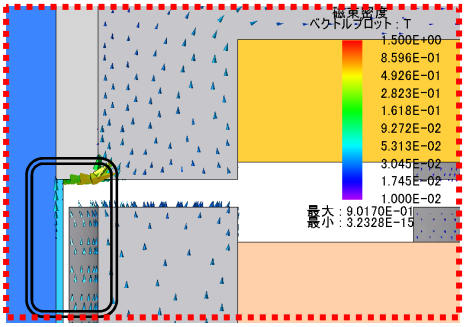

(c) With an aluminum sheet (thickness: 0.5 mm).

Fig. 4. Calculated results for the magnetic field analysis.

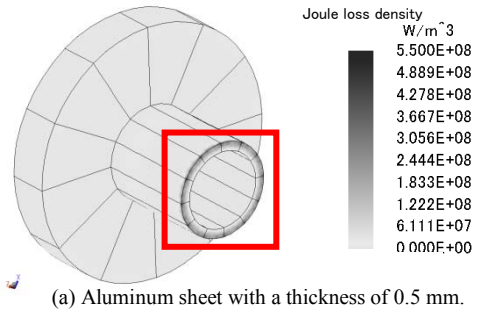

(a) Aluminum sheet with a thickness of 0.5 mm.

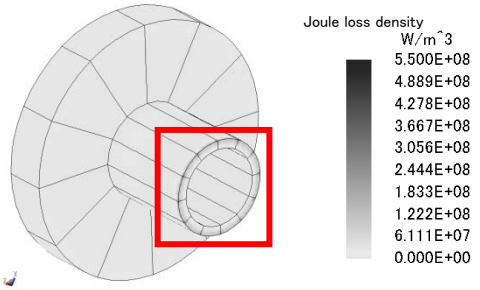

(b) Aluminum sheet with a thickness of 1.5 mm.

Fig. 5. Calculated results for the Joule loss density.

$$R_{\mathrm{LmaxS}} = kr_2\sqrt{Q_1Q_2 + \frac{Q_2^2}{k^2}} \tag{16}$$

$$\eta_{\mathrm{maxS}} = \frac{1}{1+\frac{2}{k}\sqrt{\frac{1}{Q_1Q_2}+\frac{1}{k^2Q_1^2}}} \tag{17}$$

III. MAGNETIC SHIELDING OF THE SHAFT

A. Rotary Contactless Power Transformer

Fig. 3(a) shows the exterior of the rotary contactless power transformer, and Fig. 3(b) shows the dimensions of the transformer. Table I summarizes the specifications of the transformer. The cores are made of ferrite, and Litz wires (0.1 mmφ × 800) are used for the windings. The gap of between the primary side and the secondary side of the transformer is 2

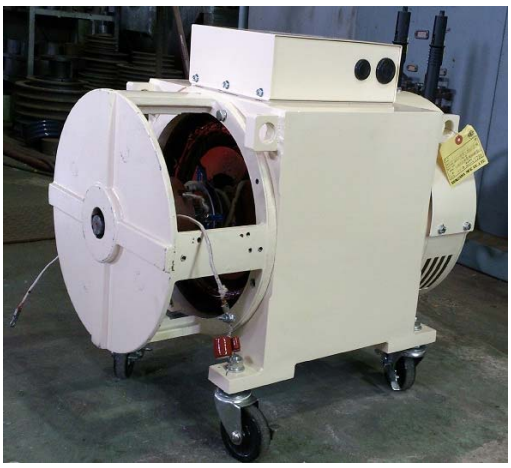

Fig. 6. 8 kW synchronous motor.

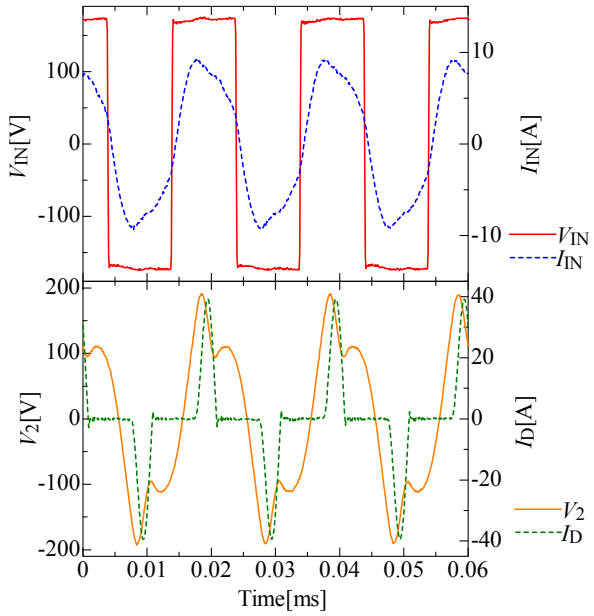

(a) SP topology (R_L = 15 Ω).

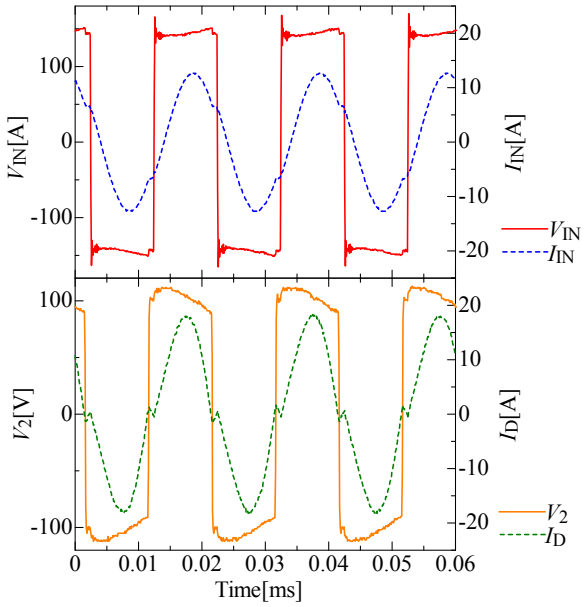

(b) S topology (R_L = 10 Ω).

Fig. 7. Input and output waveforms.

mm. Table II lists the parameters of the transformers measured by an LCR meter. The value of resonant capacitors C_P, C_S, and C_{OS} are calculated from (1), (2), and (11), respectively. Because the efficiency of the contactless power transfer system is altered by changing the gap, we also measured the transformer parameters of for gaps of 1 mm and 3 mm.

B. Magnetic Shielding of the Shaft Using an Aluminum Sheet

For a large synchronous motor, it is necessary to support both ends of the shaft of the rotor. Therefore, by placing the transformer inside of the synchronous motor, the shaft is necessary to penetrate the center of transformer. The 8 kW synchronous motor in Fig. 6 uses a carbon steel (S45C) shaft with a diameter of 25 mm. The primary transformer (transmitter) has a gap of 2.5 mm between the outer diameters of the shaft. The secondary transformer (receiver) is fastened to the shaft by bushing made of carbon steel (S45C).

A high-frequency magnetic field generated by the contactless power transfer system causes iron loss of the magnetic materials surrounding the transformers, and the transformer efficiency decreases [5], [8]. Therefore, we investigated the effectiveness of an aluminum sheet for magnetically shielding the shaft in this system. Fig. 5 shows the results of magnetic field analyses of the shaft with and without an aluminum sheet, as analyzed by the magnetic field analysis software "JMAG." The thickness of the aluminum sheet is 0.5 mm, which is thicker than the skin depth at 50 kHz. The leakage flux into the shaft from the transformers is reduced by the aluminum sheet. Thus an improvement in transformer efficiency can be realized when reducing the loss due to the leakage flux.

Furthermore, we carried out a magnetic field analysis of the shaft with a 1.5-mm-thick aluminum sheet to reduce the leakage flux into the pointed end of the bushing. Fig. 6 shows the calculated results for the Joule loss density of the bushing. We confirmed that the loss of the pointed end of the bushing is reduced by increasing the thickness of the aluminum sheet.

We performed 1 kW power transfer experiments with the S topology to confirm the effectiveness of the aluminum sheet. The inverter output frequency f_0 was 50 kHz, and the thicknesses of the aluminum sheets are 1.5 mm and 0.5 mm. The smoothing capacitor and load resistance (10 Ω) are connected to the rectifier. From the results of the experiments, the transformer efficiencies are 97.0%, 95.3%, and 92.3% with a 1.5-mm-thick aluminum sheet, with a 0.5-mm-thick aluminum sheet, and without an aluminum sheet, respectively. These results mean that the transformer efficiency is improved by the presence of the aluminum sheet for magnetically shielding the shaft, and the loss of the pointed end of the bushing is reduced by using a thicker aluminum sheet. This shielding method is effective for reducing the loss and leakage flux into the shaft in this system.

IV. Experimental Results

A. S Topology Versus SP Topology

In the S topology, the value of C_{os} is altered by load fluctuations, and the power factor of the primary side (inverter output) is lower. However, the load of the contactless power transfer system is constant for power transfer to the excitation windings of the rotor. Therefore, the S topology is useful in this case. In addition, the S topology has advantages such as compactness and no maintenance on the secondary side.

We performed 1 kW power transfer experiments for the S

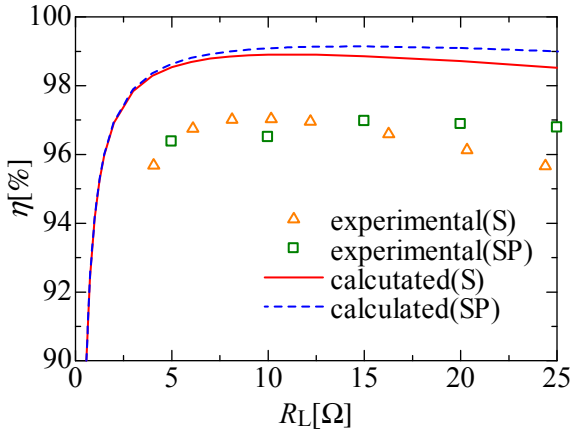

Fig. 8. Efficiency as a function of the load resistance.

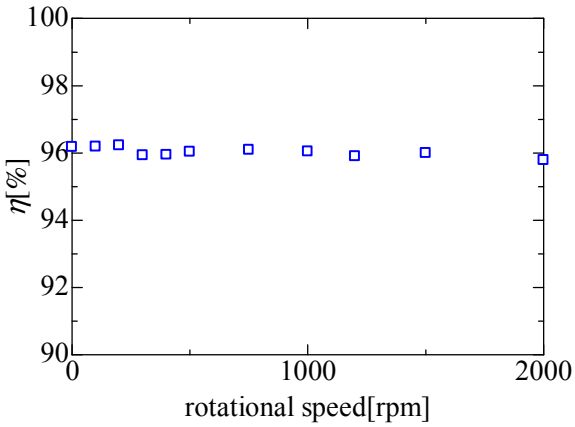

Fig. 9. Characteristics for changes in the rotational speed.

and SP topologies. The inverter output frequency f_0 was 50 kHz, and the thicknesses of the aluminum sheets were 1.5 mm. The smoothing capacitor and load resistance were connected to rectifier. Fig. 7 shows the results of experiments. In the SP topology, V_2 is a sine wave, and I_D flows into the rectifier when V_L is larger than the voltage of the smoothing capacitor. Therefore, the power factor of the secondary side is low because the time that I_D flows into the rectifier becomes short. On the other hand, I_2 flows into the rectifier at all times because V_2 of the S topology is a rectangular wave. When the system is connected to the smoothing capacitor and load resistance, the power factor of the secondary side of the S topology is higher than that of the SP topology.

B. Characteristics with a Change in the Gap Length (S Topology Versus SP Topology)

The gap between the transformers might be changed by vibration during rotation. In order to confirm the characteristics with a change in the gap length, we performed 1 kW power transfer experiments for a change in the gap length with the S and SP topologies. The inverter output frequency f_0 was 50 kHz, and the thickness of aluminum sheet was 1.5 mm. The smoothing capacitor and load resistance (10 Ω) were connected to rectifier. The gap is varied from 1 mm to 3 mm.

The results of experiments are listed in Table II. The experimental values of the transformer efficiency are lower than the calculated values because the iron loss was ignored. However, the transformer efficiencies of the two topologies are approximately constant when the gap changes from 2 mm.

C. Characteristics with a Load-Resistance Change (S Topology Versus SP Topology)

In order to confirm the characteristics with a load-resistance change, we performed 1 kW power transfer experiments with a load-resistance change for the S and SP topologies. The thickness of the aluminum sheet was 1.5 mm, and the smoothing capacitor and load resistance (10 Ω) were connected to rectifier.

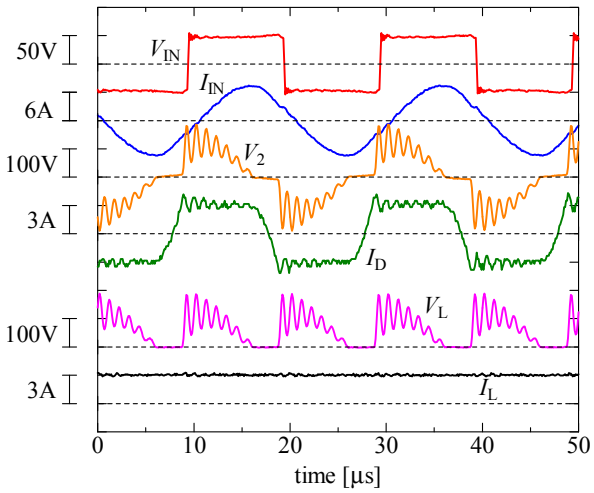

Fig. 10. Waveforms connected to the inductive load.

Figure 8 shows the transformer efficiency as a function of the load resistance. The experimental values for the transformer efficiency of the S and SP topologies are similar to the calculated curves. The experimental values of the transformer efficiency for the two topologies are at an approximately equal level. R_{Lmax} of the S topology is smaller than that of the SP topology.

D. Characteristics with a Change in the Rotational Speed (S Topology)

In order to confirm the characteristics for a change in the rotational speed, we performed 1 kW power transfer experiments for rotating secondary transformer and circuit conditions. The rotational speed was varied from 0 rpm to 2000 rpm, and the thickness of aluminum sheet was 1.5 mm. The smoothing capacitor and load resistance (10 Ω) were connected to rectifier. Fig. 9 shows the relationship between the rotational speed and the transformer efficiency. The results show that the transformer efficiencies are greater than 96% and are about same under rotating conditions. Therefore, the

transformer efficiency is not affected by the rotational speed.

E. Power Transfer to the Inductive Load (S Topology)

We performed experiments for excitation windings around the rotor of the 8 kW synchronous motor in Fig. 6. The parameters of excitation windings of the rotor are R = 20 Ω, L = 600 mH, and an excitation current of 3 A. In order to adjust the value of C_{OS} to the load resistance, C_{OS} is set to 0.063 μF. When placing a contactless power transfer system into the interior of the synchronous motor, a secondary transformer and circuit need to be constructed on the rotor side of the motor. On the secondary side, the smoothing capacitor of the rectifier is omitted, and the secondary current is smoothed by the inductance of the excitation windings. Fig. 10 shows the experimental results under excitation-current conditions (3 A, 184 W) that excite the windings of the rotor. The voltage at the excitation winding V_L is not constant owing to the omission of the smoothing capacitor. Further, the field current I_L is smoothed by the inductance of excitation windings and is constant. The input current is in phase with the input voltage, and the input power factor is 0.83. The transformer efficiency η_{TR} is 91.8%, which is lower than the case of power transfer to the load resistance (10 Ω) with a smoothing capacitor, because the resistance of the excitation windings is 20 Ω, which is shifted from R_{LmaxS}. These results reveal that the S topology is effective for power transfer to an inductive load.

V. CONCLUSION

In this paper, we proposed a resonant circuit with a primary series capacitor (S topology) for miniaturization and weight reduction of the secondary rotating part. The S topology uses only the primary series capacitor; thus the secondary circuit is compact and maintenance free. We derived η_{TRmaxS} and R_{LmaxS}, and we performed power-transfer experiments to investigate the validity of the proposed system.

The experimental results demonstrated that the transformer efficiency of the S topology is equal to that of the SP topology, and the S topology has high power factor performance at the normal gap length (2 mm). When the gap changes from 1 mm to 3 mm, the transformer efficiency remains approximately constant.

The results also showed that the transformer efficiency and power factor of the inverter output are not affected by the rotational speed or inductive load. Therefore, the S topology is effective for power transfer to an inductive load. A high efficiency of 91.8% is achieved when power is transferred to the rotor circuit of the synchronous motor.

In proposed system, an aluminum sheet for magnetically shielding the shaft is effective for reducing the loss and leakage flux into shaft.

REFERENCES

[1] J. P. C. Smeets, L. Encica, and E. A. Lomonova, "Comparison of winding topologies in a pot core rotating transformer," in *12th Int. Conf. Optim. Electr. Electron. Equip. (OPTIM)*, 2010, pp. 103-110.

[2] J. P. C. Smeets, D. C. J. Krop, J. W. Jansen, and E. A. Lomonova, "Contactless power transfer to a rotating disk," in *IEEE Int. Symp. Ind. Electron. (ISIE)*, 2010, pp. 748-753.

[3] D. Hirschmann, C. P. Dick, S. Richter, and R. W. De Doncker, "Design of contactless rotary energy transmission for an industrial application," in *IEEE Power Electron. Specialists Conf.*, 2008, pp. 4314-4319.

[4] A. Abdolkhani and A. P. Hu, "A contactless slipring system by means of axially travelling magnetic field," in *IEEE Energy Convers. Congress Expo. (ECCE)*, 2012, pp. 1796-1803.

[5] A. Abdolkhani, A. P. Hu, G. A. Covic, and M. Moridnejad, "Contactless slipring system based on rotating magnetic field principle for rotary applications," in *IEEE Energy Convers. Congress Expo. (ECCE)*, 2013, pp. 2566-2573.

[6] T. Yamanaka, Y. Kaneko, S. Abe, and T. Yasuda, "10 kW contactless power transfer system for rapid charger of electric vehicle," presented at EVS26 Int. Battery, Hybrid Fuel Cell Elect. Veh. Symp., Los Angeles, CA, May 6-9, 2012.

[7] H. Takanashi, Y. Sato, Y. Kaneko, S. Abe, and T. Yasuda "A large air gap 3 kW wireless power transfer system for electric vehicles," in *IEEE Energy Convers. Congress Expo. (ECCE)*, 2012, pp. 269-274.

[8] H. Tanifuji, R. Nozawa, Y. Kaneko, and S. Abe, "Characteristic analysis and improvement efficiency on contactless rotary transformer," in *Annu. Conf. IEEJ Ind. Appl. Soc.*, 2012, pp. I-415-I-418 (in Japanese).